ISSN(Online) : 2319 -8753
ISSN (Print) : 2347 -6710

International Journal of Innovative Research in Science, Engineering and Technology

*(An ISO 3297: 2007 Certified Organization)*

**Vol. 4, Issue 10, October 2015**

# Evolution of Microstructure during Recrystallization in As-cast Aluminium - Magnesium Alloys with Ternary Titanium/ Zirconium Addition

Abdullah Al Shafe[a], Sanjidah Akter Urmi[b], A. H. M. Azadur Rahman[b], Fahmida Gulshan[c], ASW Kurny[d]

Research Engineer, Foundry Section, Department of Metallurgy, Walton Hi-Tech Industries Ltd, Chandra, Kaliakoir, Gazipur- 1750, Bangladesh[a]

Student, Department of Materials and Metallurgical Engineering, Bangladesh University of Engineering and Technology, Dhaka-1000, Bangladesh[b]

Assistant Professor, Department of Materials and Metallurgical Engienering, Bangladesh University of Engineering and Technology, Dhaka-1000, Bangladesh[c]

Professor, Department of Materials and Metallurgical Engineering, Bangladesh University of Engineering and Technology, Dhaka-1000, Bangladesh[d]

**ABSTRACT**: The purpose of this research was to investigate the influence of Zirconium and Titanium on Al-5Mg alloy. Zirconium and Titanium in the range of 1.5-2wt% individually and combined have been added to Al-5Mg alloy by melt processing technique. The cast alloys were then subjected to investigation for their microstructure and mechanical properties.The evolution of microstructures during as cast condition was studied extensively using optical microscope (OM) which identifies the refining action of both Zr and Ti. Use of different kinds of etching reagent in the microstructural analysis showed different perspective results. The morphology of the intermetallic formed- $Al_3Zr$ and $Al_3Ti$, the presence of dendrite structures and the relation of tensile strength on secondary dendritic arm spacing were studied. Use of Zr as third party material provides greater mechanical properties compared to Ti addition but Zr does not influence hardness as does the Ti alone. Also DTA result shows the addition of Zr or Ti both increase the recrystallization temperature in different extent.

**KEYWORDS**:Al-5Mg Alloy; Optical Microscopy; Pin Dislocation; Yield Strength; Ultimate Tensile Strength; Percent Elongation, Recrystallization

## I. INTRODUCTION

Aluminium alloys that have magnesium as the chief alloying element are a group of non-heat treatable alloys possessing excellent corrosion resistance, medium strength, high ductility and weldability. Wrought Al-Mg alloys are mainly used for aerospace, automotive, marine and cryogenic applications whereas cast alloys are highly suitable forfood processing, corrosion resistance, dairy and chemical processing applications [1,2]. Alloys with low Mg content are highly formable whereas the high Mg content alloys have highercastability and high strength [3]. Solid solution strengthening is the primary strengthening mechanism that is achieved by the addition of Mg which has significant solid solubility in Al.High amount of Mg content gives strength to these alloys which is equivalent to strength of the precipitation hardening alloys. But this high concentration of Mg poses processing challenges and makes these alloys susceptible to stress corrosion cracking [3,4].

ISSN(Online) : 2319 -8753
ISSN (Print) : 2347 -6710

International Journal of Innovative Research in Science, Engineering and Technology

(An ISO 3297: 2007 Certified Organization)

Vol. 4, Issue 10, October 2015

An effective process of increasing the strength of Al alloys was first proposed by Wiley in 1971 which suggests the addition of alloying elements in Al alloys [5]. These alloys often possess small concentrations of transition elements such as scandium, manganese, zirconium or titanium to increase the strength of the alloy by grain refinement [6]. Addition of these transition metals causes theirtrialuminides to formthat have low solubilities and diffusion coefficient thatcontrol the evolution of grain, subgrain structure, grain coarsening during subsequent processing operations and increase the recrystallization temperature [7-9]. Influence of the transition elements in the increasing of the recrystallization temperature is according to the order Zr>Ti>Mo>Nb>Cr>Mn>V [10]. Addition of Zrcauses the $Al_3Zr$ particles to precipitate in the Al matrix [10].These particles possess high melting points compared with that of Al matrix and because of this, these particles are coherent and have superior thermal stability. Additionally, their stability against grain coarsening and redissolution cause a more even distribution of dislocations and pin grain boundaries. More than 0.1% addition of Zr causes $Al_3Zr$ particles to form as a primary phase from the melt during rapid solidification which act as nuclei for the solidification of Al. Thus Zr causes grain refining operation of Al [7,11-13]. Addition of Ti during thermal processing causes $Al_3Ti$ intermetallic phase to form in situ which is intrinsically stable with a melting point of 1623 K [14,15]. This high melting point along with low density of about 3.3 $Mg/m^3$ and slowest diffusivity in Al (e.g. diffusivity $3.0\times10^{-19}$ $m^2s^{-1}$ and $3.2\times10^{-17}$ $m^2s^{-1}$ at 500°C and 600°C respectively) make these strengthening dispersoids particularly suitable and resistant to coarsening which is a very important for strength retention at high temperature [14].

Our purpose of this study was to observe the microstructural changes of as cast Al-5 weight% Mg alloy after the addition of 2 weight% Zr and 2 weight% Ti both individually and jointly and then relate the microstructural change to the mechanical properties. Thermal analysis was also conducted by Differential Thermal Analysis and the results were further differentiated to get the better understandings of recrystallization behavior

## II. MATERIALS AND TEST PROCEDURE

### A. Casting Procedure:

Alloys with chemical compositions given in the table 1 were used in this paper. Aluminum was introduced as a precursor bar form and magnesium was taken in ribbon form. Zirconium and titanium were taken in as nano-powder.

**Table 1:**
Alloy Compositions (balance Al)

| Alloy | Weight % of Mg | Weight % of Zr | Weight % of Ti |
|---|---|---|---|
| Alloy 1 | 5 | | |
| Alloy 2 | 5 | 2 | |
| Alloy 3 | 5 | | 2 |
| Alloy 4 | 5 | 2 | 2 |

Melting of the alloys was done in a clay-graphite crucible furnace fired by natural gas using fluxing agent. The melt temperature was monitored with a chromel-alumel (type K) thermocouple. The temperature of the melt was raised to almost 800-900$^o$C and kept at that temperature for some time and stirred with an alumina rod for about 30 seconds. During this time, sufficient amount of degasser was added in the melt. Degasser used was mainly comprised of Ammonium Chloride ($NH_4Cl$). After the Skimming off the impurities, melt was poured in the metal mold preheated to almost 200$^0$C.

### B. Microstructural Analysis:

For microstructural analysis, two etching reagents were used and the results obtained using them were compared. Etching reagent 1 contains following components

1. 75 ml distilled water
2. 15 ml Hydrogen Fluoride (HF)
3. 10 ml Hydrochloric Acid (HCl)

Etching reagent 2 contains contains

1. 25 ml $CH_3OH$

ISSN(Online) : 2319 -8753
ISSN (Print) : 2347 -6710

International Journal of Innovative Research in Science, Engineering and Technology

(An ISO 3297: 2007 Certified Organization)

Vol. 4, Issue 10, October 2015

2. 25 ml HCl
3. 25 ml $HNO_3$
4. 1 drop HF

Microstructures of the samples were then observed using an optical microscope (OPTIKA, ITALY, B-600 MET).

**C. Tensile Test:**

Tensile test was conducted at room temperature using INSTRON 3369 universal testing machine. Samples were cut according to the DIN standard and tested in a common strain rate $10^{-3}$ $S^{-1}$. In each alloy at least 3 samples were tested and then average values were taken.

**D. Hardness Test:**

Rockwell hardness was measured using Rockwell hardness testing machine (FR-IE, Future Tech. Corporation, Tokyo, Japan. All hardness measurements were performed on blocks of greater than 5 mm thickness using F scale. The blocks for hardness measurement were ground using 600 µmSiC paper prior to hardness measurements. A 1/16 inch steel ball indenter was used. A load of 60 kgf was applied for a period of 15 s.

**E. Thermal analysis:**

Thermal analysis was done in order to study the phase transformations during various stages of the heat treatment. TG/DTA 6300 (Model – EXSTAR 6000, SII, Seiko Instrument Inc.) was used to evaluate the thermal behavior of the samples. The analysis was carried out in nitrogen atmosphere at heating rate of $20^0$C/min. Small samples 10-15 mg of each alloy were heated up to 600°C. Then small samples were placed on the sample holder of the device. The reference holder was left blank. Prior to each measurement the whole heating unit was cooled down. The samples were heated up to 600°C at a heating rate of 20°C/min, and then slowly cooled down. The temperature difference between an inert (Alumina) reference and the sample was recorded and mass loss was calculated from the thermogravimetric curve. Phase transformation is accompanied by a release (exothermic) or absorption (endothermic) of thermal energy. An exothermic event results in a sudden increase in dT/dt value, whereas an endothermic event results in a sudden decrease in dT/dt value at the starting point of the transformation.

## III. RESULTS AND DISCUSSIONS

**A. Microstructural Analysis Using Etching Reagent 1:**

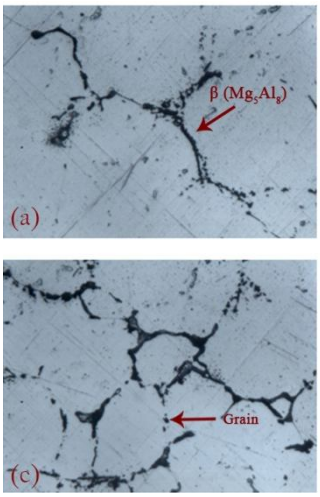


Figure 1: Microstructure of Alloy 1 (Al-Mg), Magnification: 200x

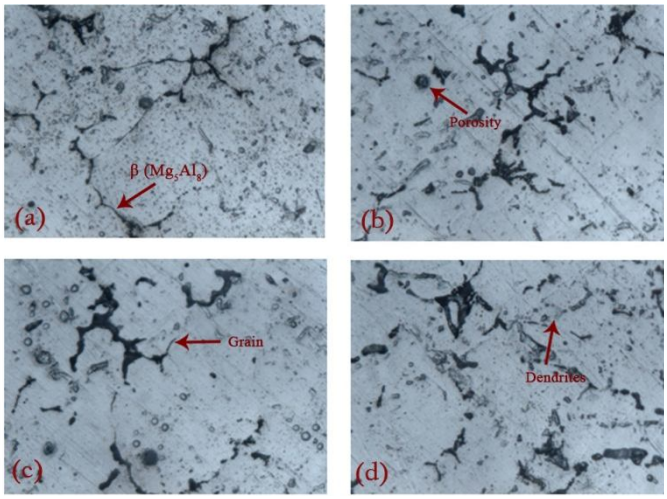


Figure 2: Microstructure of Alloy 2 (Al-Mg-Zr), Magnification: 200x

Figure 1 shows different features of alloy 1 microstructure. Alloy 1 consists of Al and Mg. Figure 1(a) shows eutectic or β phase ($Al_8Mg_5$) as the flakes. Figure 1(b) shows porosity. Porosity may occur for various reasons, such as

ISSN(Online) : 2319 -8753
ISSN (Print) : 2347 -6710

International Journal of Innovative Research in Science, Engineering and Technology

(An ISO 3297: 2007 Certified Organization)

Vol. 4, Issue 10, October 2015

casting defects, surface oxidation, bad polishing etc. Figure 1(c) shows grains in the structure and also the grain boundary. Figure 1(d) shows the dendrites formed during solidification of the liquid Al-Mg alloy.

Figure 2 shows different features of alloy 2 microstructure. Alloy 2 consists of Al and Mg and a small addition of Zr. Figure 2(a) shows eutectic or β phase ($Al_8Mg_5$) as flake structure. Figure 2(b) shows porosity while figure 2(c) shows grains in the structure and also the grain boundary. Figure 2(d) shows the dendrites formed during solidification of the liquid Al-Mg-Zr alloy.

Addition of Ti in Al Mg alloy introduces alloy 3. Figure 3 shows the optical microstructure of alloy 3. Figure 3(a) shows the β phase ($Al_8Mg_5$) along with dendrite structure. Grain and grain boundaries are seen easily in figure 3(b). Figure 3(d) clearly shows the porosity caused in the structure. Grain size can be determined from the figure. So it is not possible to compare the grain refining action of Zr and Ti by optimizing these microstructures. Also presence of $Al_3Ti$ cannot be identified by the figure. Better microstructural analysis is necessary to interpret the details of structure.

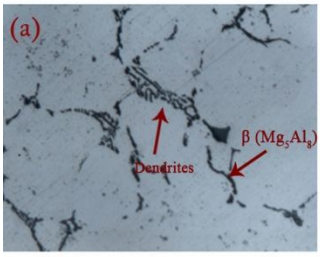


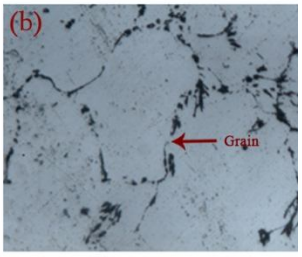


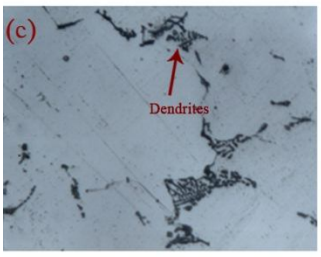


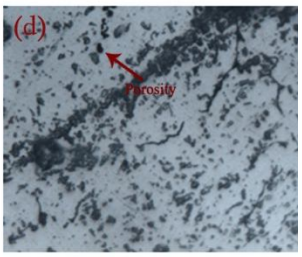


Figure 3: Microstructure of Alloy 3 (Al-Mg-Ti), Magnification: 200x

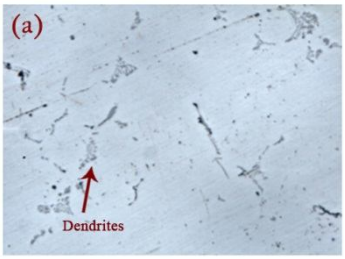


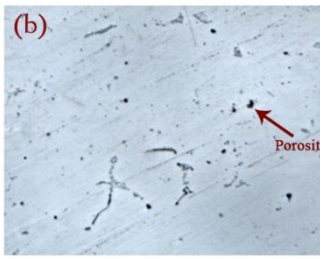


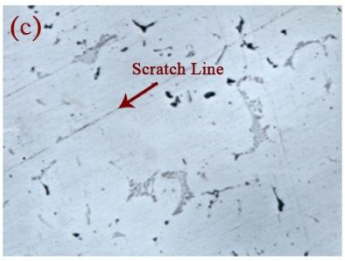


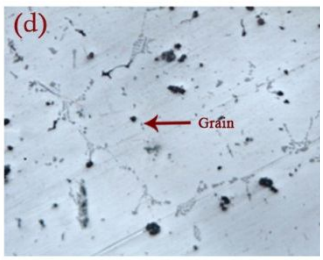


Figure 4: Microstructure of Alloy 4 (Al-Mg-Zr-Ti), Magnification: 200x

Different features of alloy 4 microstructure are shown in the above figure 4. Alloy 4 consists of Al and Mg and a small addition of both Zr and Ti. Figure 4(a) shows the dendrite structure. But no $Al_3Zr$ or $Al_3Ti$ can be identified from the figure. Figure 4(b) shows porosity. Figure 4(c)shows scratch lines due to bad polishing. Figure 4(d) shows the grains in the structure and also the grain boundary.

**B. Microstructural Analysis Using Etching Reagent 2:**

Use of etching reagent 2 has provided significant microstructural analysis providing dendrite structure. This etching reagent reveals very clearly the primary and secondary dendrite structure and also some other microstructural features like secondary dendrite arm spacing, porosity etc.Measurement of the secondary dendrite arm spacing (SDAS) can be used to measure tensile strength or elongation theoretically.

Figure 5 shows different features of alloy 1. Figure 5(a) and 5(c) shows the primary dendrites which appear due to rapid solidification. Figure 51(b) shows the secondary dendrite growth from the primary dendrites. Figure 5(d) shows clearly the secondary dendrite arm spacing (SDAS).

Figure 6 shows different features of alloy 2. Figure 6(a) shows the dendrite structure. Figure 6(b) shows the porosity. Figure 6(c) shows the primary and secondary dendrite growth. Figure 6(e) shows clearly the SDAS

ISSN(Online) : 2319 -8753
ISSN (Print) : 2347 -6710

International Journal of Innovative Research in Science, Engineering and Technology

(An ISO 3297: 2007 Certified Organization)

Vol. 4, Issue 10, October 2015

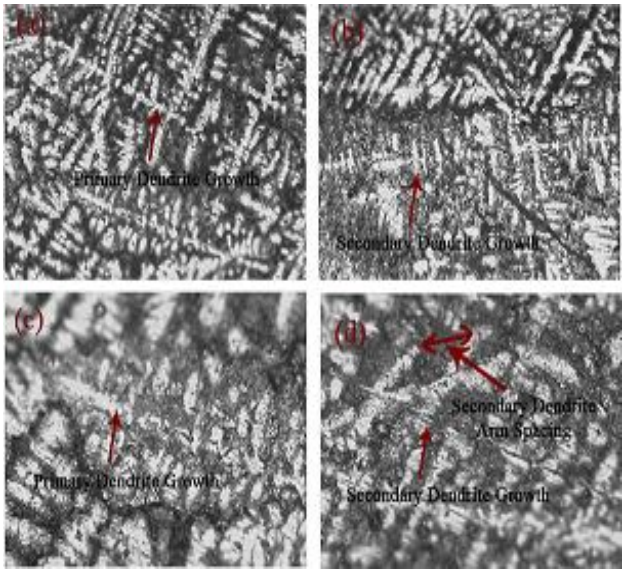


Figure 5: Microstructure of Alloy 1 (Al-Mg), Magnification: (a,b) - 100x (c,d)- 200x

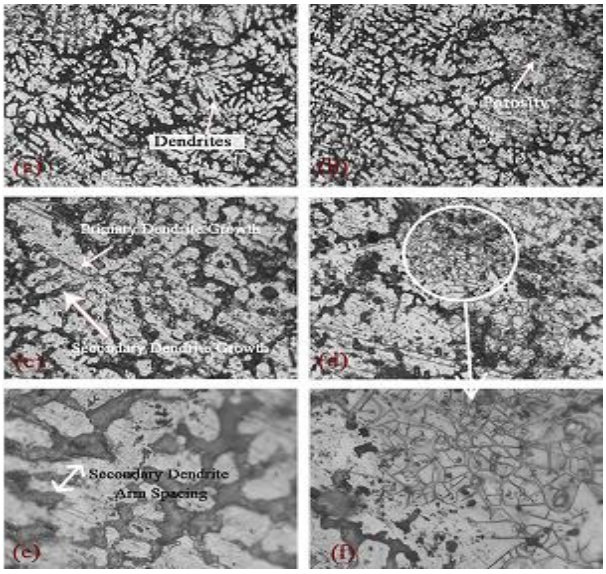


Figure 6: Microstructure of Alloy 2 (Al-Mg-Zr), Magnification: (a,b)- 100x, (c,d)- 200x, (e,f)- 500x

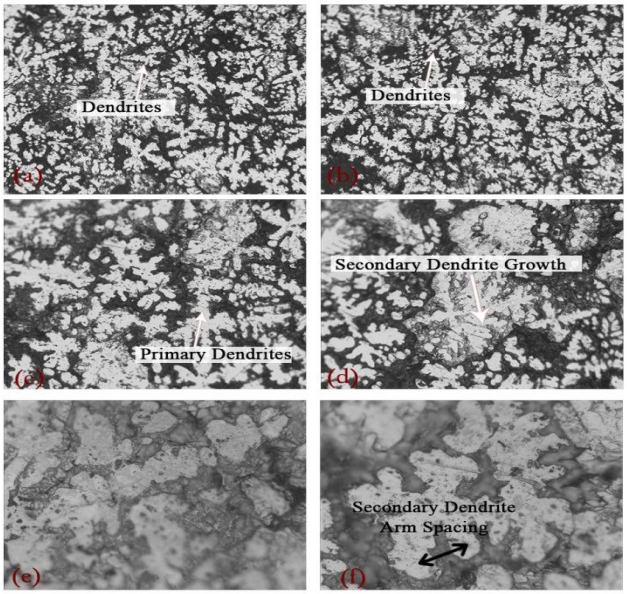


Figure 7: Microstructure of Alloy 3 (Al-Mg-Ti), Magnification: (a,b)-100x, (c,d)-200x, (e,f)-500x

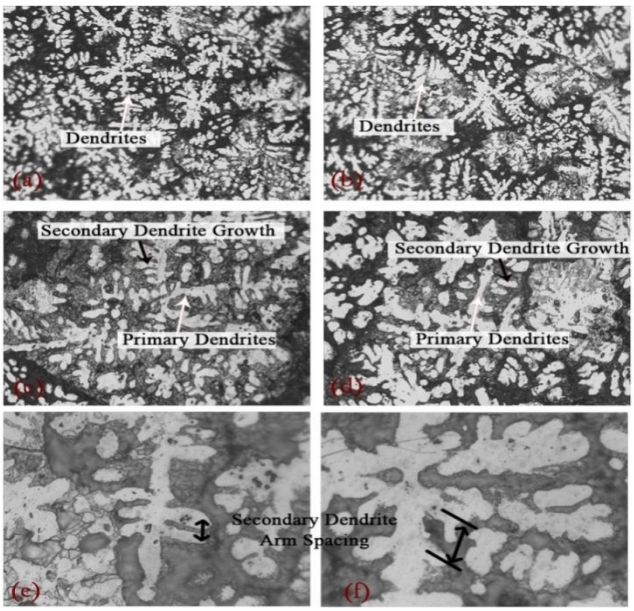


Figure 8: Microstructure of Alloy 4 (Al-Mg-Zr-Ti), Magnification: (a,b)-100x, (c,d)-200x, (e,f)-500x

Figure 7 shows different aspects of alloy 3. Figure 7(a) and 7(b) shows the dendrite structures. Figure 7(c), 7(d) reveals the primary and secondary dendrite growth respectively while figure 7(f) shows the SDAS.

Figure 8 shows the microstructures of alloy 4. In the figures, figure 8(a) and 8(b) shows the dendrite structure. Figure 8(c) and 8(d) shows the primary and secondary dendrite growth. Figure 8(e) and 8(f) shows the secondary dendrite arm spacing.

ISSN(Online) : 2319 -8753
ISSN (Print) : 2347 -6710

International Journal of Innovative Research in Science, Engineering and Technology

(An ISO 3297: 2007 Certified Organization)

Vol. 4, Issue 10, October 2015

The calculated SDAS for alloy 1 to alloy 4 are shown in Table 2 and their average valuesare shown and compared in figure 9.

**Table 2**
Secondary Dendrite arm spacing for alloy 1 to alloy 4

| Alloy | Measurement 1 (cm) | Measurement 2 (cm) | Measurement 3 (cm) | Measurement 4 (cm) | Average (cm) |
|---|---|---|---|---|---|
| Alloy 1 | 0.0085 | 0.006 | 0.0045 | 0.005 | 0.006 |
| Alloy 2 | 0.0025 | 0.0025 | 0.003 | 0.0025 | 0.002625 |
| Alloy 3 | 0.0025 | 0.002 | 0.002 | 0.003 | 0.002375 |
| Alloy 4 | 0.002 | 0.0035 | 0.0015 | 0.002 | 0.00225 |

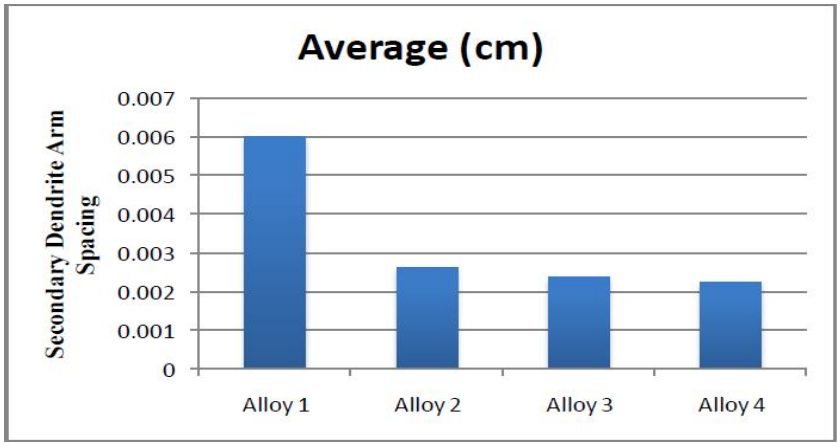


Figure 9: Variation of Secondary Dendrite arm spacing for alloy 1 to alloy 4

SDAS valueswere calculated by determining the distance between peak to peak or valley to valley in the secondary dendrite arms. The distance was then divided by the magnification number providing the result in centimeter (cm) unit. From the table 2 and figure 9, the largest average SDAS value is for alloy 1, while the smallest value is for alloy 4 containing Zr and Ti along with Mg in pure Al. So it can be said that, grains are much smaller in alloy 4 than alloy 1 hence SDAS is lower in this alloy. Also, alloy 2 and 3 has smaller values (very close to alloy 4) of SDAS. So, alloy 2 and 3 also has very small grain sizes. But combined effect of Zr and Ti in alloy 4 is not greatly increased compared to alloy 2 and 3. Overall interpretation can be standardized as, the grain refining action of third element like Zr or Ti individually is greater than combined action of them. Also, SDAS is smaller in alloy 3 than alloy 4 attributing better result of Ti addition than Zr addition.

**C.Chemical Analysis:**

**Table 3:** Chemical composition of alloys after using flux

| Alloy | Fe (%) | Mg (%) | Ti (%) | Zr (%) | Si (%) | Mn (%) | Al(%) |
|---|---|---|---|---|---|---|---|
| Remelt Alloy 1 | 0.41 | 5.23 | - | - | 0.12 | 0.01 | Balance |
| Remelt Alloy 2 | 0.33 | 4.72 | - | 0.14 | 0.06 | 0.01 | |
| Remelt Alloy 3 | 0.44 | 5.11 | 0.15 | - | 0.19 | 0.01 | |
| Remelt Alloy 4 | 0.44 | 4.86 | 0.14 | 0.08 | 0.07 | 0.01 | |

ISSN(Online) : 2319 -8753
ISSN (Print) : 2347 -6710

International Journal of Innovative Research in Science, Engineering and Technology

(An ISO 3297: 2007 Certified Organization)

Vol. 4, Issue 10, October 2015

**D. Tensile Properties:**

Figure 10(a) shows the Ultimate Tensile Strength results. It was revealed that alloy 4 has the best ultimate tensile strength of 204.433 MPa followed by alloy 1 with ultimate tensile strength of 182.4 MPa which is more than the values obtained for alloy 3 and alloy 2 with ultimate tensile strengths of 181.0667 and 137 respectively. The abrupt increase of UTS in alloy 4 can be attributed due the combined effect of Zr and Ti trialuminides. Both of $Al_3Zr$ and $Al_3Ti$ provide grain refining by pinning effect. These particles provide obstacles against grain boundary movements. The decrease of UTS in alloy 2 and alloy 3 can be explained by the nonuniform distribution of $Al_3Zr$ and $Al_3Ti$ particles. From the figure it can be obtained that grain refining action of Ti is greater than Zr as $Al_3Ti$ provide better grain refinement.

Factors affecting UTS also affect yield strength of alloys. Yield strength of different alloys has been shown in figure 10(b). From the figure, yield strength is higher for alloy 2 containing Zr, followed by alloy 4, then alloy 1 and last of all alloy 3.

Figure 10(c) shows the elongation of the four alloys. Percentage elongation or ductility was the highest for alloy 1 and lowest for alloy 3. Since Zr and Ti precipitates increases the strength of alloys, it substantially also reduces the ductility. Sudden abrupt decrease in elongation for alloy 3 can be demonstrated by the defects in the testing setup along with structure of the alloy. Ti provides better grain refinement than Zr as can be stated by UTS values, but it reduces elongation as well. Al3Ti is very coherent with Al matrix and thus provide it lower elastic energy of the coherent interface. Their smaller grain size and lower misfit also reduces elastic energy hence ductility decreases.

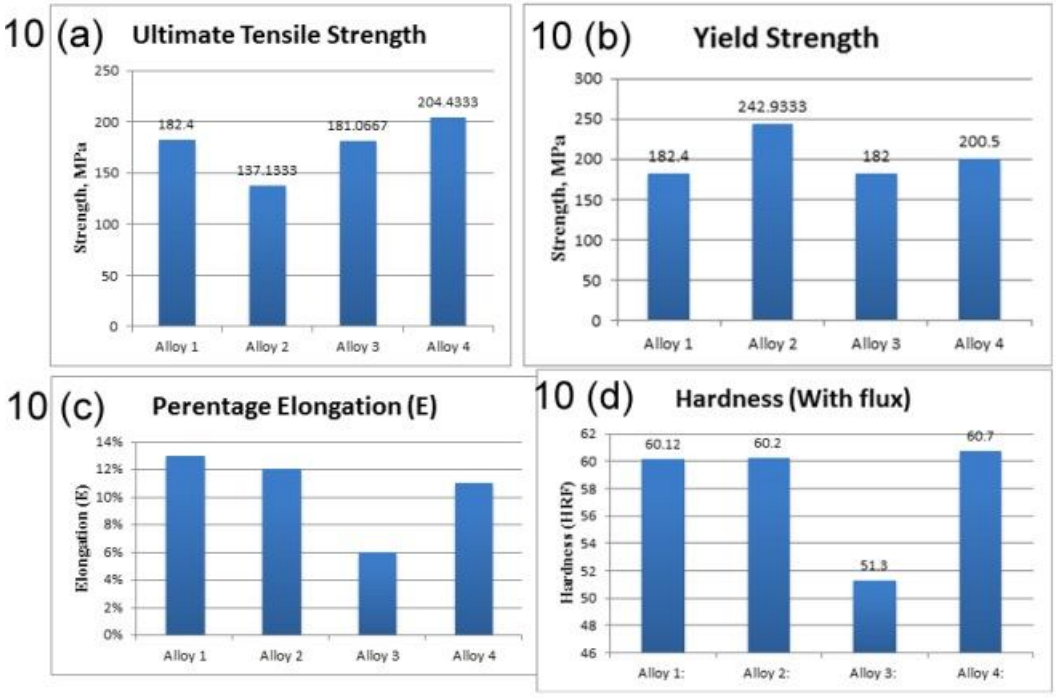


Figure 10: (a) variation of ultimate tensile strength for alloy 1 to alloy 4; (b) variation of yield strength for alloy 1 to alloy 4; (c) different percentage elongation (average value) for different alloys; (d) variation of hardness of alloy 1 to alloy 4

**D. Hardness Test:**

Figure 10(d) shows the hardness values of the four alloys where alloy 4 has the highest hardness value followed by alloy 2. Alloy 4 has both Zr and Ti addition in the structure. Hence $Al_3Zr$ and $Al_3Ti$ intermetallic compounds are both present in the structure. Both of these intermetallic compounds are hard and from coherent particles with grain boundaries. They inhibit the propagation of grain boundary sliding. All of these criteria increase the hardness of alloy 4

ISSN(Online) : 2319 -8753
ISSN (Print) : 2347 -6710

International Journal of Innovative Research in Science, Engineering and Technology

(An ISO 3297: 2007 Certified Organization)

Vol. 4, Issue 10, October 2015

among all of the other alloys. On the other hand, unexpected large decrease of hardness in alloy 3 can be attributed to the inhomogeneous distribution of $Al_3Ti$ particles.

**E. Thermal analysis**

DDTA graph for different alloys obtained from the analysis is shown below in figure 11. Figure 11 shows the variation of recrystallization temperature of different alloy samples. In DTA curves endothermic reactions show valley while exothermic reactions show peaks. In the differentiation (DDTA) the endothermic reactions show peaks and exothermic show valley. Recrystallization is an endothermic reaction as it requires energy to proceed. The energy necessary for recrystallization is smaller compared to other structure phase mechanisms such as melting or fusion or sintering. As a result, in DTA curves there evolve very little range of valleys indicating the recrystallization. Hence the DDTA analysis is taken and recrystallization range portion is extrapolated. Figure 11 shows the results of extrapolation of DTA curve. From the figure we can see that, Al with 5% addition of Mg has a recrystallization temperature of $579.2^0$C which is smaller than other 3 alloys. Highest recrystallization temperature obtained was for alloy 3, containing Ti. But according to theory, we have stated earlier that, Zr increases recrystallization temperature higher than Ti. The theory is somewhat contradictory with the results obtained in here.

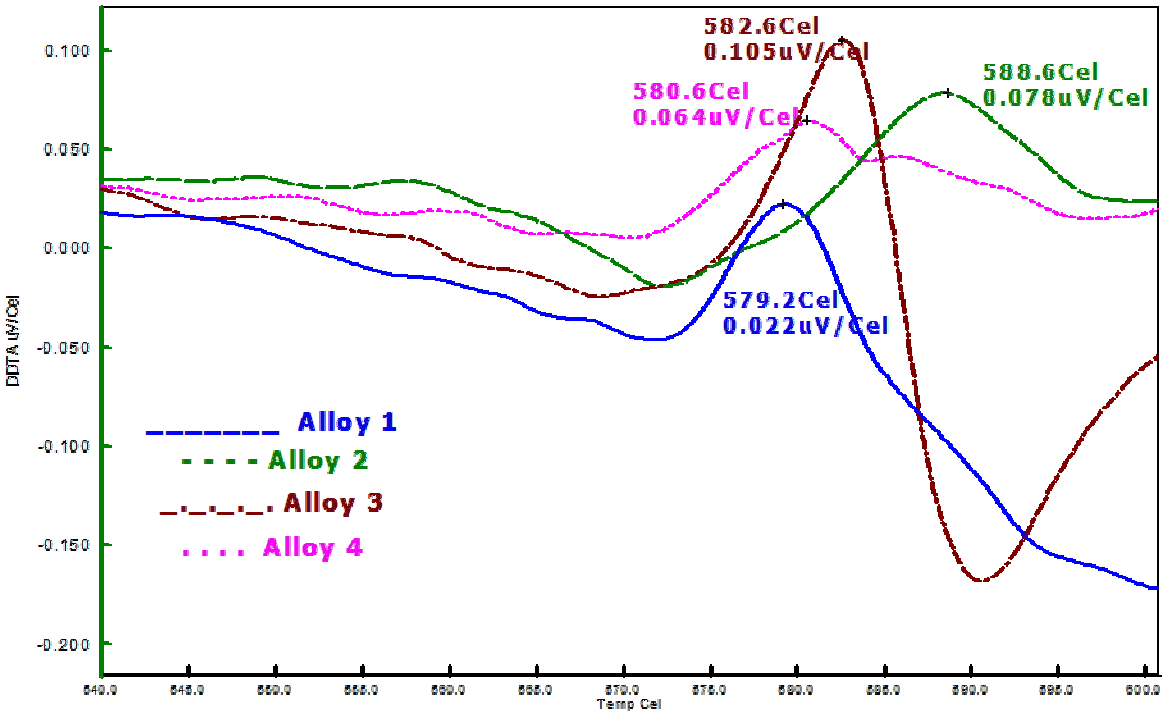


Figure 11: DDTA curves for alloy 1 to alloy 4

## IV. CONCLUSION

Test results have revealed that, Al-Mg alloy solidifies as dendrites and the mechanical properties of the alloy depend on the extent of dendrites formed in the structure. Tensile properties and percent elongation decreases as the secondary dendrite arm (SDAS) increases while decrease in SDAS increases them. Addition of Zr and Ti refines the grains of Al-Mg alloy. Refining action of Ti is greater than Zr. Secondary dendrite arm spacing is very large for alloy containing only Al-Mg, but much low for alloys containing Zr or Ti or both. Ultimate tensile strength reaches to the highest after the combined addition of Zr and Ti. But yield strength of combined addition is somewhat lower than Zr addition alone. Percentage elongation and ductility decreases with the addition of Zr or Ti or both. Ti reduces much ductility than Zr while combined action of Zr and Ti is higher than Ti alone. Combined action of Zr and Ti addition increases hardness

ISSN(Online) : 2319 -8753
ISSN (Print) : 2347 -6710

International Journal of Innovative Research in Science, Engineering and Technology

(An ISO 3297: 2007 Certified Organization)

Vol. 4, Issue 10, October 2015

than any other alloys tested.Ti increases recrystallization temperature individually then Zr or Zr and Ti combined.No eutectic temperature range was observed in the DDTA curves. Only recrystallization temperature range was found. Addition of Zr or Ti or both increases recrystallization temperature but Ti increseas higher than Zr. Combined action of Zr and Ti is lower than Ti or Zr addition alone.

## V. ACKNOWLEDGEMENTS

The authors thank Bangladesh Council of Scientific and Industrial Research (BCSIR) authority for giving access to their laboratory facilities. We express our thanks and gratitude to Dr. M. A. Gafur, Project Director, "Development of Materials for Tools and Biometallic implant", PP & PDC, BCSIR for his valuable advice. We are especially indebted to Engr. Md. RakibulQadir (PP &PDC, BCSIR, Dhaka), for his continuous help, suggestions and also for helping us understanding the basic theories of this work.

## REFERENCES

[1]Lathabai, S., Lloyd,P.G.,"The effect of scandium on the microstructure, mechanical properties and weldability of a cast Al–Mg alloy", ActaMaterialia, 50, 4275-4292, 2002.
[2]Vijayan,S.,Raju,R.,Subbaiah,K.,Sridhar,N.,Rao,S. R. K.,"Friction stir welding of AL-MG alloy optimization of process parameters using Taguchi method", Experimental Techniques, 34, 37–44, 2009.
[3]Watari,H.,Haga,T.,Shibue,Y.,Davey,K.,Koga, N.,"Twin roll casting of magnesium alloys with high aluminum contents", Journal of Achievements in Materials and Manufacturing Engineering, 18, 419-422, 2006.
[4]Jones,R. H. D.,Baer, R.,Danielson, M. J.,Vetrano, J. S.,"Role of Mg in the stress corrosion cracking of an Al-Mg alloy", Metallurgical and Materials Transactions A, 32A, 1699-1711, 2001.
[5]Willey, L.A., inventor; Aluminum Company of America, assignee. Aluminum Scandium Alloy. US patent 3,619,181. 1971 November 9.
[6]Hughes, A. E.,Birbilis, N.,Mol, J. M.C.,Garcia, S. J.,Zhou,X., Thompson,G. E.,"High Strength Al-Alloys: Microstructure, Corrosion and Principles of Protection, Recent Trends in Processing and Degradation of Aluminium Alloys", Prof. Zaki Ahmad (Ed.), 2011, ISBN: 978-953-307-734-5.
[7]Mahmoud,A.E.,Mahfouz,M. G.,Gad- Elrab, H. G.,"Influence of Zirconium on the Grain Refinement of Al 6063 alloy", Int. Journal of Engineering Research and Applications, 4, 188-194, 2014.
[8]Cavaliere,P.,Cerri, E.,Leo,P.,"A Study of the Response of a Zr-modified 2014 Aluminium Alloy Subjected to Fatigue Loading", Materials Forum, 28, 172-177, 2004.
[9]Clouet, E., Barbu, A., La, L.,Martin,G.,"Precipitation kinetics of Al3Zr and Al3Sc in aluminum alloys modeled with cluster dynamics", Acta Mater. ,53, 2313-2325, 2005.
[10]Meng, Y., Zhao, Z.,Cui, J., "Effect of minor Zr and Sc on microstructures and mechanical properties of Al−Mg−Si−Cu−Cr−V alloys", Trans. Nonferrous Met. Soc. China, 23, 1882−1889, 2013
[11]Mahmudi, R.,Sepehrband, P.,Ghasemi, H. M.,"Improved properties of A319 aluminum casting alloy modified with Zr", Materials Letters, 60, 2606-2610, 2006.
[12]Robson, J.D., Prangnell,P.B.,"Modelling Al3Zr dispersoid precipitation in multicomponent aluminium alloys", Materials Science and Engineering: A, 352, 240–250, 2003.
[13]Park, S. Ill,Han, S. Z.,Choi, S. K.,Lee, H. M.,"Phase Equilibria of Al(Ti,V,Zr) Intermetallic System",ScriptaMaterialia, 34, 1697-1704, 1996.
[14]Cavaliere,P., "Effect of friction stir processing on the fatigue properties of a Zr modified 2014 aluminium alloy", Materials Characterization, 57, 100–104, 2006.
[15]Barlow,I. C.,Jones,H.,Rainforth,W. M., "Evolution of Microstructure and Hardening, and the Role of Al3Ti Coarsening, During Extended Thermal Treatment in Mechanically Alloyed Al-Ti-O Based Materials", Actamaterialia, 49, 1209–1224, 2001.
[16]Dobrzański, L.A.,Labisz, K.,Olsen,A., "Microstructure and mechanical properties of the Al-Ti alloy with calcium addition", Journal of Achievements in Materials and Manufacturing Engineering, 26, 183-186, 2008.